Better Separations for Proteins and Peptides

by

Ling Li

B.S. Nanjing University, 2003

Submitted to the Graduate Faculty of

Arts and Science in partial fulfillment

of the requirements for the degree of

Master of Science

University of Pittsburgh

2008

UNIVERSITY OF PITTSBURGH

Graduate Faculty of Arts and Science

This thesis was presented

by

Ling Li

It was defended on

May 19, 2008

and approved by

Dr. Adrian Michael, Professor, Department of Chemistry

Dr. Shigeru Amemiya, Professor, Department of Chemistry

Dr. Stephen G. Weber, Professor, Department of Chemistry

Thesis Director: Dr. Stephen G. Weber, Professor, Department of Chemistry

Better Separation for Proteins and Peptides

Ling Li, M.S.

University of Pittsburgh, 2008

In recent years, determination of proteins and peptides has been gaining more popularity. However, one-dimensional separation systems cannot always offer sufficient sensitivity or selectivity, especially for more complex samples. Two-dimensional separation systems can provide more peak capacity by coupling two orthogonal separation methods together. To achieve better two-dimensional separation, two conditions must be satisfied: 1. the two coupled separation methods should have different separation mechanisms, so called orthogonal; 2. the second dimensional separation method should be much faster than the first dimension to ensure that more effluent from the first dimension be transferred to the second dimension. Capillary electrophoresis, with its different separation mechanism from HPLC, and its high separation speed, serves as a good candidate as the second dimension separation method when HPLC serves as the first dimension separation method. In addition, chip electrophoresis is more advantageous to us due to its faster speed and more efficiency compared to capillary electrophoresis. Therefore, we would like to set up a two-dimensional separation system with the first dimensional HPLC separation followed by the second dimensional chip electrophoresis separation.

As for HPLC, elevated temperature is utilized to increase the separation speed. The viscosity of the solvent is related to temperature in such a way that higher temperature leads to lower viscosity. The diffusion coefficient of the solute is therefore decreased based on Stokes-

Einstein equation ($D_m = \frac{RT}{6r\eta N_{Av}}$). As a result, higher linear velocities can be achieved with regular pressure. It is suggested that diffusion coefficient plays such an important role in affecting the separation speed that efforts are deserved to investigate how diffusion coefficient changes with temperatures. In our experiment, we would like to determine the diffusion coefficients of several peptides and compare the experimental values with estimation values from various empirical equations.

TABLE OF CONTENTS

LIST OF TABLES

LIST OF FIGURES

PREFACE

First and Foremost, I would like to thank my advisor, Prof. Stephen G. Weber, for offering me great chance to carry out the interesting projects. He patiently guided me and encouraged me throughout my academic program.

I would like to express my gratitude to my committee members, Prof. Adrian Michael and Prof. Shigeru Amemiya for their kind assistance during my comprehensive exam.

I am also thankful to Weber group, especially peptide group, for their helpful suggestions and continuous encouragement in my research work.

I would also like to thank Electronic shop and Machine shop for their help and patience.

In addition, I would like to thank National Institutes of Health for generous financial support.

1.0 INTRODUCTION

1.1 BETTER SEPARATION

In recent years, better separation, especially for more complex biological samples, becomes more and more necessary. Over the past few years, many efforts have been made towards this end. In this context, we will focus on multi-dimensional separation and high temperature chromatography, both of which enhanced the separation efficiency and resolution over traditional one-dimensional separation method.

1.2 MULTI-DIMENSIONAL SEPARATION

Several decades ago, multi-dimensional separation techniques, which have better selectivity and resolution over individual one-dimensional separation, were developed. The separation power of the separation systems is best expressed by peak capacity (this concept will be discussed in details in the following context). For example, for the separation of peptides and proteins, the peak capacities achieved in multi-dimensional separations (> 1000) are much higher than the highest peak capacities obtained in one-dimensional separation (400 – 1000). [1-4]

1.2.1 Introduction of multi-dimensional separation

The earliest work of multi-dimensional separation was performed by Martin along two axes of a sheet of filter paper (two dimensional (2D) chromatography × chromatography) in 1944.[5] Later, chromatography × electrophoresis[6, 7] and electrophoresis × electrophoresis[7] separations were also used by other researchers.

In 1984, Giddings proposed that "2D separations are those techniques in which a sample is subjected to two displacement processes oriented at right angles to one another".[8] In the mean while, several other groups made considerable contributions to the development of the 2D technology. For example, O'Farrel and co-workers[9] coupled two modes of gel electrophoresis (isoelectric focusing and SDS polyacrylamide gel electrophoresis) together. This system is capable of resolving 1100 proteins. Also, Zakaria[10] et al. utilized 2D LC through separation in the first column followed by the elution in the second column.

Up to now, a variety of separation mechanisms have been coupled in multidimensional separation, and very high peak capacities have been achieved.

Theory:

As mentioned before, the resolution power of a multi-dimensional system is best expressed by peak capacity[8], which was introduced by Giddings in 1967. It is defined as "the maximum number of separated peaks that can be fit (with adjacent peaks at some specified resolution value taken as 1.0 in all equations below) into the path length or space provided by the separation method".[11] According to Giddings' peak capacity theory, the peak capacity of a comprehensive multi-dimensional separation ($n_{c,iD}$) equals to the product (not the sum) of the

peak capacities of the component one-dimension step (${}^{1}n_c, {}^{2}n_c ... {}^{i}n_c$), when the separation mechanism in each dimension is orthogonal.

$$n_{c,iD} = {}^{1}n_c \times {}^{2}n_c \times ... \times {}^{i}n_c$$

Therefore, the resolving power of multi-dimensional separations is greatly enhanced over one-dimensional separations under ideal conditions.

In a multi-dimensional separation system, a sample is first separated in the first dimension, and the effluent is further separated by at least one more method. In principle, the more dimensions of methods are coupled together, the higher resolving power can be obtained. However, due to the practical constrains, the majority of the reported multi-dimensional systems are 2D systems.

2D separation can be conducted by colleting the effluent from the first dimension, and then transporting it to the second dimension for further separation, which is considered as "off-line system"; or by connecting the two dimensions with tubes, valves or columns to ensure direct transfer of the first dimension effluent to the second dimension, which is referred to as "on-line system".

In off-line systems, effluent collection enables sample treatment before the second dimension separation, thus optimization of the system becomes relatively easier compared to on-line systems. On the other hand, on-line systems enable direct transport of the sample into the second dimension, which shortens the experiment time. While both off-line and on-line systems have their own advantages, most of the research is focused on the on-line 2D systems.

For the on-line systems, the effluent transfer makes the interface connecting the first and second dimensions very important. If the complete sample is separated and analyzed in all dimensions, the system is considered as comprehensive[12]. However, if only one fraction of the

sample from the first dimension is separated in the second dimension, the system is called a heart-cut system[13].

Regardless of off-line or on-line, comprehensive or heart-cut systems, two criteria, which were set out by Giddings[8, 11], have to be met for ideal separations. First, the separation mechanisms should be orthogonal, which means the separation mechanism for each dimension must be totally independent of each other. For example, reversed-phase liquid chromatography (RPLC), whose separation mechanism is based on hydrophobicity, is orthogonal to capillary zone electrophoresis (CZE), whose separation mechanism is based on difference in the electrophoretic mobility of the analytes. Second, no resolution achieved in the first dimension may be lost in any subsequent dimension. To achieve this, the second dimension should be much faster than the first dimension, so that after a portion of the effluent from first dimension is injected into the second dimension, the analysis in the second dimension can be finished before the next injection. Murphy *et al*[14] demonstrated that 3-4 fractions of the width of a first dimension peak must be collected to prevent the resolution or peak capacity loss in the 2D systems, which further stresses the necessity for very fast second dimension separations.

1.2.2 Typical 2D systems

The most commonly used techniques for peptide separation are high performance liquid chromatography (HPLC) and capillary electrophoresis (CE). Combinations of various modes of HPLC (normal-phase: NP, reversed-phase: RPLC, ion exchange: IEC, size exclusion: SEC, affinity) and CE (capillary zone: CZE, capillary isoelectric focusing: CIEF, capillary gel electrophoresis: CGE, isotachophoresis: ITP, affinity, micellar electrokinetic chromatography:

MEKC) are used in 2D systems. These 2D systems are generally classified into three categories: LC-LC, LC-CE and CE-CE systems.

LC-LC system:

The various modes of HPLC offer a lot of possible combinations for 2D LC-LC systems. In these systems, valves or columns are usually utilized to transfer the effluent from the first dimension to second dimension. However, some problems arise from the liquid transfer:

(1) There might be solvent incompatibility of the mobile phase between the first dimension and second dimension systems. This means, the solvents for the two dimensions should not be immiscible. Otherwise, different strategies should be developed to solve this problem. For example, Sonnefeld and co-workers transferred the sample of interest from the first dimension to a packed column, in which the solvent of the trapped sample was removed by gas and the sample was desorbed by another solvent for further separation in the second dimension.[15]

(2) The transfer of the analytes through the valve or column introduces extra band broadening. This can be solved by sample pre-concentration prior to transferring to the second dimension.

(3) The second dimension LC should be much faster than the first dimension, if comprehensive separation is desired. Therefore, various methods, such as the application of monolithic columns[16-19] and elevated temperatures[4, 20-25] have been used to accelerate the second dimensional LC.

An example of the LC-LC systems is a comprehensive IEC-RPLC system which was developed by Jorgenson and co-workers[26] to separate peptides from porcine adrenal gland. The two LC systems are connected with an eight-port valve equipped with two sample loops. In this

system, a whole separation completes in 32 h, with high sensitivity (3-16 pmol) and resolution being achieved.

CE-CE system:

With different CE modes coupled together, orthogonal 2D CE systems are also possible. However, the low injection volume in CE will result in a sensitivity problem for the second dimension. Normally when a low concentration sample is injected, large volume has to be used to enhance its sensitivity. Due to the low injection volume in both dimensions, this is not applicable in CE-CE systems. Therefore, samples can be pre-concentrated by field amplification[27, 28] or sample stacking[27, 28], or more sensitive detectors can be used to reach better detection[29, 30].

An example of CE-CE system is the 2D CZE-CGE system which was devised by Sweedler and co-workers[31] for the analysis of some target peptides, a tryptic digest of trypsinogen and an individual B2 neuron from the marine mollusk *Aplysia californica*.

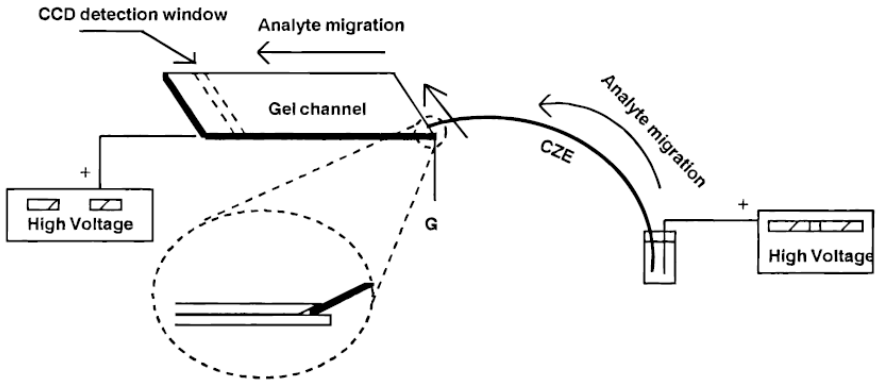

Figure 1. Schematic diagram of the CZE-CGE separation system showing the CZE capillary, gel channel, interface, and the power supply arrangement.[31]

In this system, the second dimensional CGE separation is equipped with several gel-filled channels which serve as parallel separation capillaries. As depicted in Figure 1, after the sample is separated in the first dimension CZE, the end of the CZE capillary is moved across the entrances of the gel-filled channels so that multiple injections will be accomplished in the second dimension and several CGE separations can be performed in parallel. Therefore, comprehensive sample separation is achieved.

LC-CE system:

Since Giddings' criterion states that best multidimensional separation is achieved when two systems with totally different separation mechanism are coupled, LC-CE system was therefore a reasonable combination which is generally more orthogonal than LC-LC or CE-CE systems. Capillary electrophoresis, a faster method than HPLC, is no doubt a very good candidate to couple with HPLC. As a result, we would like to set-up an HPLC-CE system in our laboratory.

There are some problems associated with the LC-CE systems:

(1) As stated before, the injection volume of CE is extremely small. As a result, the large difference between the injection volume between LC (μL range) and CE (nL range) makes comprehensive analysis of samples more complicated. This problem can be solved by using a T-piece, through which a majority of the sample goes to the waste while a small part of sample goes to CE. In this case, the second dimension CE must be sensitive enough to diminish the effect of the material loss during the transfer process. Alternatively, nano LC, which has comparable injection volume as CE, can be used instead of the regular LC column.[32] However,

this will result in a tremendous sensitivity loss in the first dimension. Thus other approaches are required to solve this problem.

2) The voltage applied in CE might have some influence on the first dimension LC detection, when electrochemical detector is used in LC. This problem can usually be addressed by using an electrical decoupler to isolate the detector from the separation voltage.[4, 33, 34] More interestingly, Lunte and co-workers developed an electrically isolated potentiostat, which uses digital communication with an on-board microcontroller to control all the analog signal and isolate the separation voltage. [35]

The first LC-CE system was developed by Jorgenson and co-workers[36, 37] in 1990. They used a regular LC column in the first dimension and a sample loop as the interface. While micro LC columns are more suitable than regular LC columns for small sample analysis because of their higher separation efficiency and increased mass sensitivity, transfer of the small volume effluent from the micro columns to the second dimension becomes problematic due to extra band broadening. Therefore, Jorgenson designed an interface to couple SEC with CZE (Figure 2)[32].

As illustrated in Figure 2a, the SEC column and the electrophoresis capillary are connected by a home-made flow gating interface which consists of two stainless steel plates with a 125 μm Teflon gasket in between. The expanded view of the center region of the flow gating interface is shown in Figure 2b, in which the SEC column is coupled with a fused-silica connecting tubing through a piece of Teflon tubing. The fused-silica tubing directly faces the inlet of CZE capillary, which is separated only by the thickness of the Teflon gasket. The gasket has a 1-mm channel cut in it, through which flush buffer passes to control the injection of the SEC effluent into the CZE capillary. Normally the CZE buffer is flushed from the top of the flow

gating interface to the bottom, which at the same time prevents the SEC effluent from entering the CZE capillary. The injection is hence realized when the buffer flow is interrupted.

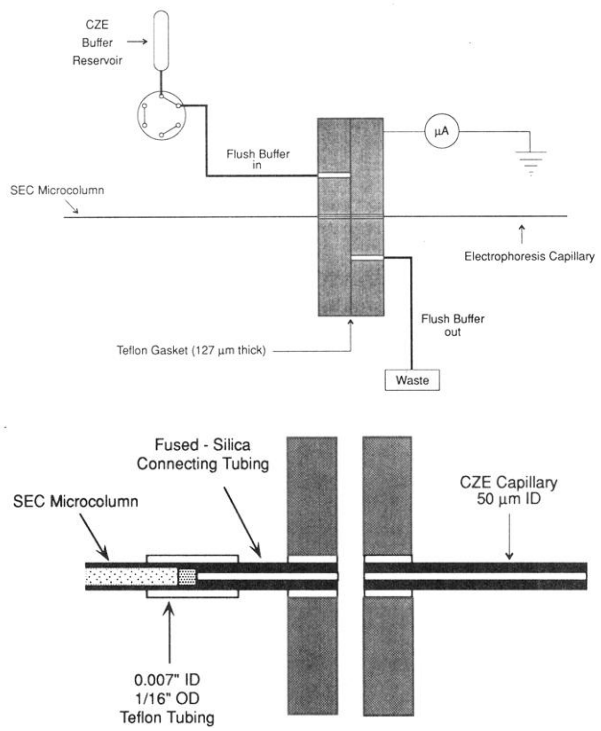

Figure 2. a) Schematic view of instrumental setup for 2D SEC-CE using a Transverse Flow Gating Interface; b) expanded view of the central region of the flow gating interface. [32]

In general, multi-dimensional separation systems offer higher sensitivity and peak capacities which enable more efficient analysis for complex biological samples. Our purpose of the experiment is to set up an HPLC-CE system, and we have carried out some preliminary work on the interface of the 2D system which will be discussed in Chapter 2.

1.3 HIGH TEMPERATURE CHROMATOGRAPHY

1.3.1 Fast liquid chromatography

The overall goal of separation is to achieve sufficient selectivity and resolution within the shortest time. A lot of researchers, especially Guiochon, Knox, Horvath and Poppe, made tremendous contributions, which help us in better understanding of the factors that limit the speed in HPLC. [20, 28, 38-45]

Based on Knox equation, which is a reduced form of plate height equation, the column performance can be evaluated:

$$h = A \cdot v^{1/3} + \frac{B}{v} + C \cdot v \tag{1}$$

$$\frac{h}{v} = A \cdot v^{-2/3} + \frac{B}{v^2} + C \tag{2}$$

Where h and v stand for the reduced plate height and reduced velocity, respectively.

Also, in 1980 Guiochon[39] introduced the following equation which clearly reveals the relationship between the analysis time and other chromatographic parameters:

$$t_{analysis} = N \cdot \frac{1+k'}{D_m} \cdot \frac{h}{v} \cdot d_p^2 \tag{3}$$

In this equation, N is the required column efficiency, k' is the retention factor of the last eluting peak, D_m is the analyte's diffusion coefficient in the mobile phase, and d_p is the packing material particle diameter.

For fast separation where v becomes very large, it is more reasonable to focus on $\frac{h}{v}$ rather than h itself. We assume that when v is large enough, term C in equation 2 becomes dominant, and the first two terms (A & B terms) become negligible. As a result,

$$\frac{t_{analysis}}{N} = C \cdot \frac{1+k'}{D_m} \cdot d_p^2 \qquad (4)$$

This equation tells us that the time required to generate one plate is proportional to the square of the packing material particle diameter with other parameters (column length, eluent linear velocity, column temperature, etc.) being constant. In other words, with smaller particle diameter, faster analysis can be achieved.[46] However, when other conditions such as column length, eluent linear velocity and column temperature remain constant, the use of smaller particle size requires the increase of pressure, which is limited to the highest pressure that the pump can provide and the resulting back pressure that valves, columns and injector, etc can endure. Therefore, other methods are needed for fast separation.

In addition, these equations don't give the direct correlation between the separation efficiency and the speed in HPLC.

1.3.2 Poppe plots

In 1997, Poppe introduced the Poppe plots, which help us a lot to understand reveal the correlation of speed with separation efficiency.[41] Also, poppe plots are widely used for the selection of proper column parameters (e.g., particle size and column length) under specified conditions (e.g., maximum N at a given analysis time).

In Poppe plot, the logarithm of the "plate time" (H/u or t_0/N) is plotted against the logarithm of the plate number (N). And the plot is generated as follows: the chromatographic parameters, such as the particle size, maximum pressure, and temperature, are set. For a chosen plate number N_r, the u_0 value was increased successively to calculate the resulting plate height H, the column length L, and the resulting pressure. When the resulting pressure reaches the maximum pressure, the iteration ends, and the maximum value of u_0 is thus found. The generated plot is represented in Figure 3.

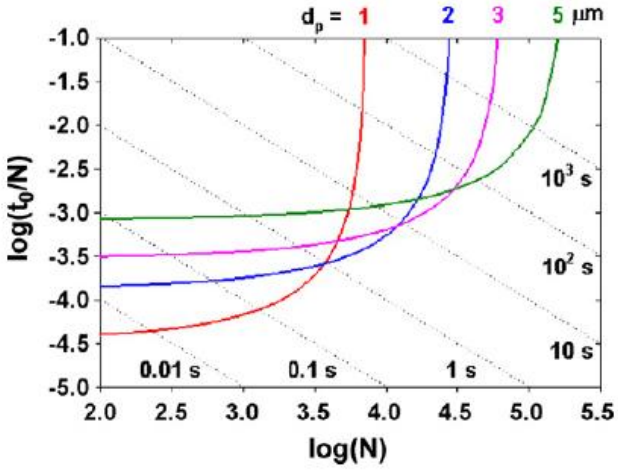

Figure 3. Poppe plot for packed bed columns with different particle sizes.

Conditions: $\Delta P = 400 bar$, $T = 40^{\circ}C$, $\phi = 500$, $\eta = 0.69 cP$, $D_m = 1\times10^{-5}\, cm^2/s$. Coefficients in reduced van Deemter equation were: $A = 1.04$, $B = 15.98$ and $C = 0.033$. Each dotted line represents a constant column dead time. [47]

As shown in Figure 3, there are a set of dotted lines which represent different dead time (t_0). The reason is that, when N is multiplied by H/u_0 ($= t_0/N$), the unretained time t_0 is obtained. Since the Poppe plot is logarithmic, each constant dead time turns out to be a straight

line in the plot. Furthermore, the lower left of the plot represents faster separation while the upper right part refers to slower separation but with higher *N* values, from which we can come to the conclusion that fastest separation time and highest *N* value cannot be accomplished simultaneously. This means, compromise must be made between the analysis time and resolution.

1.3.3 Effect of elevated temperature on HPLC

Based on equation 3, the speed of the system is also dependent on diffusion coefficient D_m. According to Stokes-Einstein equation (equation 5) in which D_m is related to the temperature of the system and the viscosity of the solvent, it is absolutely true that the temperature (T) can influence the speed of HPLC system.

$$D_m = \frac{RT}{6r\eta N_{Av}} \tag{5}$$

In Equation 5, R, T, r and N_{Av} represent the gas constant, temperature (K), radius of the diffuser (assumed spherical), and Avogodro's number, respectively. Since these four parameters are temperature independent, we lump them into a constant (= $1/\Omega$), and Equation 5 is substituted into Equation 4 to form a new equation:

$$\frac{t_{analysis}}{N} = \Omega \cdot C \cdot \frac{1+k'}{T} \cdot \eta \cdot d_p^2 \tag{6}$$

This equation suggests that with higher temperature and lower eluent viscosity, less time is needed to generate one plate.

It is also well known that there is a strong relationship between temperature (T) and viscosity (η). For example, the viscosity in different acetonitrile-water (ACN/water) mixtures can be calculated using the following equation[48]:

$$\eta = 10^{(-2.063+(602/T)+0.071\cdot X_{ACN}+(62/T)\cdot X_{ACN}+0.504\cdot X_{ACN}^2-(346/T)\cdot X_{ACN}^2)} \quad (7)$$

In Equation 4, T is the temperature in Kelvin, and X is the volumetric fraction of ACN in the mixture.

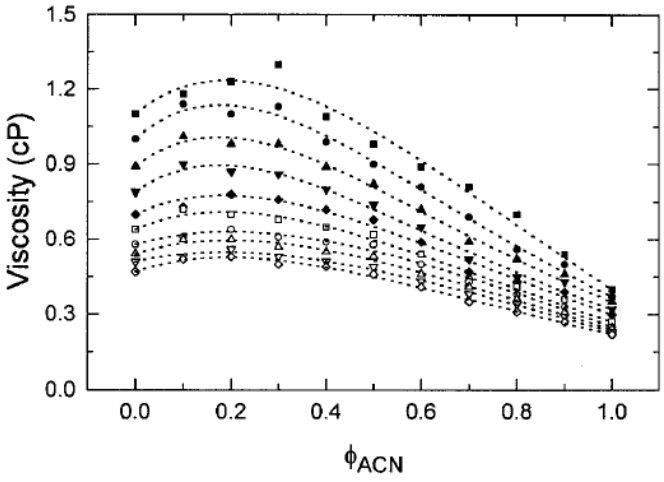

Figure 4. Effect of mobile phase composition (acetonitrile/water) and temperature on viscosity. Temperature from top to bottom: 15; 20; 25; 30; 35; 40; 45; 50; 55; 60.[49]

Figure 4 graphically shows the dependence of viscosity on temperature and mobile phase composition (ACN/water mixture) based on Equation 7.[49] It is obvious that there is a maximum viscosity at certain mobile phase composition. Meanwhile, as temperature rises, e.g., from 25 ℃ to 60 ℃, the viscosity for the mixture decreases by a factor of 2.

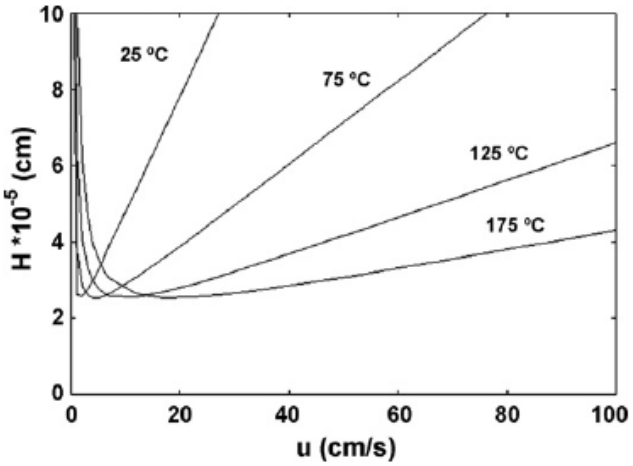

Figure 5. Plots of reduced plate height against the reduced velocity scaled to $D_{m,25}$ with the temperature as the parameter. Conditions: totally porous particles, rapid sorption kinetics, $D_{m,25} = 6 \times 10^{-7}$ and $d_p = 3\mu m$.[42]

Through theoretical calculation, Horvath[42] demonstrated that by increasing temperature, the optimum velocity increases, and the limiting slope at high velocities decreases, when the column parameters, such as plate count, retention and pressure drop are held constant (Figure 5). Therefore, with higher temperature, viscosity decreases and diffusion increases. As a result, higher linear velocities can be achieved with regular pressure. Later Yan and co-workers[23] proved Horvath's predictions, and the results are illustrated in Figure 6. However, from both Figure 5 and Figure 6, the increase of temperature does not result in the decrease of the minimum value of H.

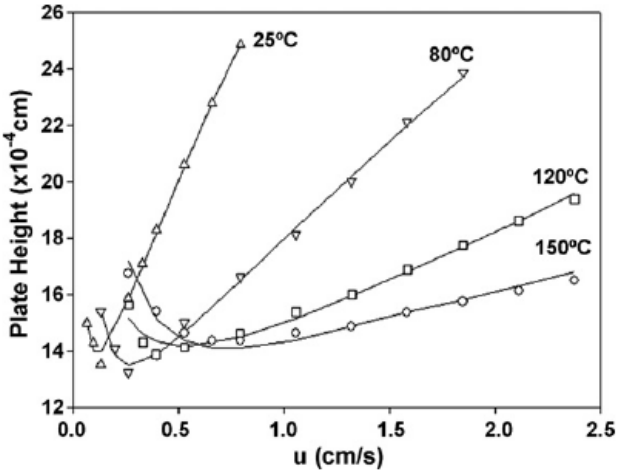

Figure 6. Plate height versus linear velocity at various temperatures.[42]

Furthermore, Hancock and co-workers[50-52] studied the selectivity of peptides and proteins on sterically protected C8 and C18 columns at different temperatures and with mobile phase compositions, with the conclusion that high temperature is able to improve the selectivity.

Although elevated temperature leads to higher separation speed and better selectivity, the high temperature liquid chromatography are not very widely used due to the following problems:

First, the silica-based stationary phases are unstable at high temperature. This problem can be solved by using thermally stable stationary phases which can stand up to 200 ℃.

Second, a large temperature mismatch between the incoming eluent and the column (> 5 ℃) will cause severe band broadening and peak splitting as pictured in Figure 7.[45, 53-55] Therefore, pre-heating of the incoming eluent is performed.

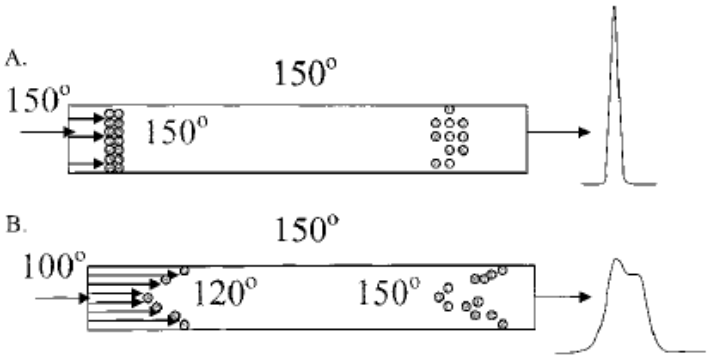

Figure 7. Schematic view of the effect of the eluent-column temperature mismatch. (A) No eluent-column temperature mismatch leads only to column and extracolumn broadening. (B) The eluent is not fully thermally equilibrated. The cool eluent produces a radial gradient in retention factor and viscosity, thereby broadening the band and destroying peak shape and efficiency.[45]

Third, the analyte might be unstable at high temperature. However, in fast separation, we just need to ensure that the analytes are stable within the time of the chromatography run. And Carr and co-workers confirmed that most of the analytes are thermally stable during the on-column residence times of 10-20s. [20, 42, 46, 56]

In conclusion, elevated temperature can be widely used in HPLC to improve both separation speed and selectivity. However, the diffusion coefficients used in the chromatography are usually estimated by correlation equations such as the Wilke-Chang equation. In Chapter 3,

we would like to experimentally determine the diffusion coefficients of peptides to evaluate the accuracy of the correlation equations.

2.0 ZIPTIP EXPERIMENT

2.1 BACKGROUND

As discussed in Chapter 1, new approaches are needed to solve the volume difference problem in LC-CE systems.

In LC-LC and CE-CE systems, pre-concentration is usually (sometimes) performed in order to increase the concentration of the trace level analytes to reach the detection limit of the detector. In the various pre-concentration methods, solid phase extraction (SPE) is most frequently used. [57-61]

SPE is able to solve two problems: first, it can be used to concentrate the analytes. The analytes are retained in the sorbent followed by the elution of the analytes with a smaller amount of elution solvent; second, impurities can be removed. Therefore, SPE is a potential candidate in the LC-CE interface so that the analytes can be transferred from the first dimensional LC to the second dimensional CE with reduced volume and increased concentration.

In our experiment, we would like to use the Ziptip® pipette tips (C18 resin) as a SPE model to test whether it can efficiently retain the analyte – Cu(II)-peptides complex (the postcolumn derivatization product from the first dimension LC system), and then elute the complex with organic solvent. If this is accomplished, the C18 resin will be used in the interface of our LC-CE system so that comprehensive 2D separation can be achieved.

2.2 MATERIALS AND METHODS

2.2.1 Materials

The organic solvents used in this experiment, acetonitrile (ACN) and 4-methylmorpholine, were of analytical grade and purchased from Sigma (St. Louis, MO). Water for all studies was purified with Milli-Q system (Millipore Synthesis A10, Billerica, MA). Trifluoroacetic acid (TFA) and Leu-Enkephalin were both purchased from Sigma (St. Louis, MO). All other compounds were of analytical grade and purchased from commercial sources. The Ziptip® pipette tips used for the sample treatment were obtained from Millipore (Billerica, MA).

2.2.2 Preparation of samples

The peptide solutions were prepared by dissolving Leu-Enkephalin (YGGFL) in milli-Q water with 0.1 % TFA at approximately milli-molar concentrations.

The derivatization solution (Cu(II) solution) contains 2.0 mM $CuSO_4$, 12.0 mM Na_2Tar (sodium tartrate), 0.24 M Na_2CO_3 and 0.24 M of $NaHCO_3$ in milli-Q water.

The Cu(II)-YGGFL solutions were prepared by mixing the peptide solution and Cu(II) solution in a 1:1 volume ratio.

2.2.3 Sample treatment

The Cu(II)-YGGFL samples were treated as follows (Figure 8):

(1) Rinsing: Attach the Zip-tip column to an Eppendorf pipet. Carefully withdraw 10 μL of ACN to rinse the Zip-tip column, and then dispense it.

(2) Adsorption: Carefully withdraw and dispense the Cu(II)-YGGFL solution 10 times to ensure complete adsorption of complex to the resin. Store the resulting solution in Vial A.

(3) Elution: Carefully withdraw and dispense the "elution solution" 10 times so that the adsorbed complex can be thoroughly washed out. Store the solution in Vial B.

(4) Washing: Carefully withdraw the "wash solution", and dispense it to Vial C.

(5) Repeat step (2)-(4) until enough solutions were collected for UV detection.

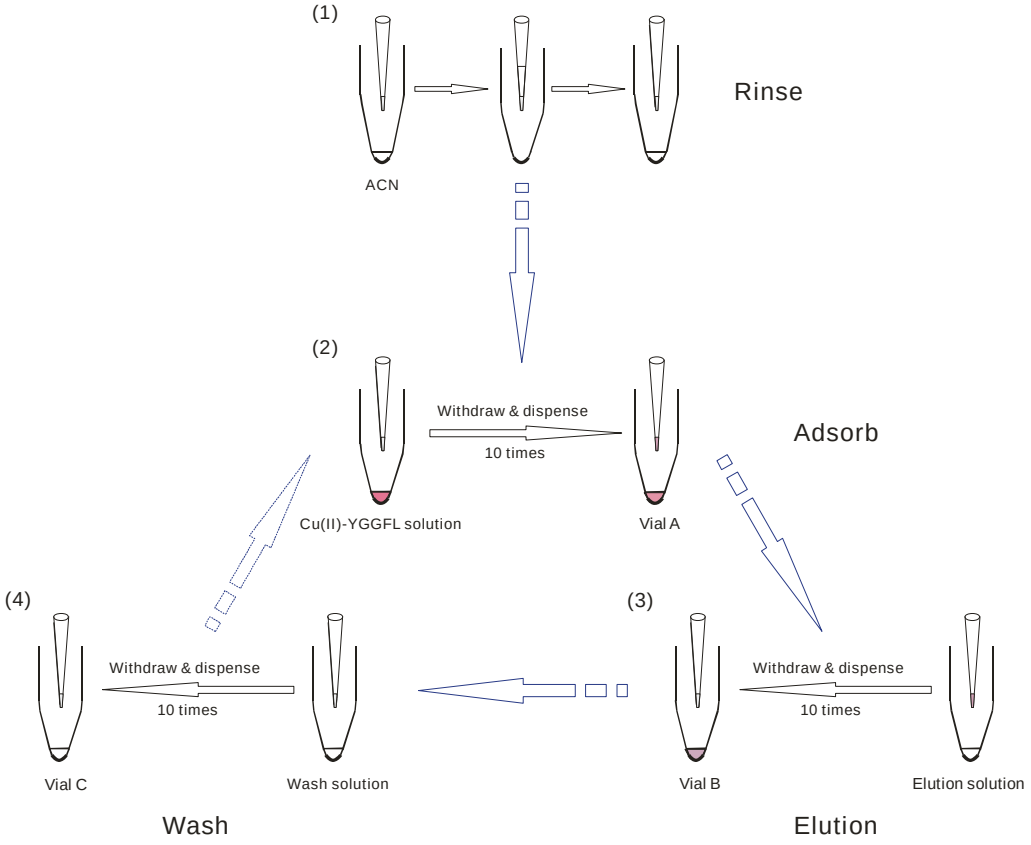

Figure 8. Sample treatment procedure.

However, during the experiment, different compositions of solutions were used. Therefore, two terms: “wash solution” and “elution solution”, which will be specified in the later context, were used in the sample treatment.

2.2.4 UV detection

The samples were detected with a Hewlett-Packard 8453 UV-Vis Spectrometer. Data collection and analysis were performed with 8453 UV-Vis system software.

2.3 RESULTS AND DISCUSSION

2.3.1 Condition 1

In this experiment, two different concentrations of peptide solutions (0.1 mM and 0.2 mM) were investigated. At first, we chose 0.1 % TFA in milli-Q water as the “wash solution”, and the 1:1 mixture of ACN and “wash solution” (0.1 % TFA in milli-Q water) as the “elution solution”.

The UV results show that, under these conditions, the peptide YGGFL was retained to the C18 resin and was washed out with very good elution efficiency. (Table 1)

Table 1. The washed out percentage and elution efficiency of YGGFL complex.

	Washed out percentage*	Elution Efficiency*
0.1 mM Cu(II)-YGGFL	96.9 %	96.9 %
0.2 mM Cu(II)-YGGFL	85.2 %	102 %

Note: Washed out percentage* $= \frac{conc_{SolutionC}}{origconc} \times 100\%$

Elution efficiency* $= \frac{conc_{SolutionC}}{conc_{orig} - conc_{solutionA} - conc_{solutionB}} \times 100\%$

As shown in Table 1, 100 % and 82.9 % of YGGFL (for 0.1 mM Cu(II)-YGGFL solution and 0.2 mM Cu(II)-YGGFL solution, respectively) were adsorbed to the C18 resin of the ziptip. Although the elution efficiency is extremely high, it didn't meet our expectation that Cu(II)-YGGFL complex be retained followed by the elution. The reason why Cu(II)-YGGFL complex dissociates during the process is that both the "wash solution" and "elution solution" are acidic, in which the Cu(II)-YGGFL complex is unstable. Accordingly, we changed the experiment conditions to Condition 2.

2.3.2 Condition 2

In order to eliminate the dissociation of the Cu(II)-YGGFL complex, "wash solution" and "elution solution" were changed to milli-Q water and ACN, respectively, both of which are neutral. At this time, Cu(II)-YGGFL complex were washed out from the resin. However, the resulting elution efficiency is not satisfactory.

Table 2. The washed out percentage and elution efficiency of Cu(II)-YGGFL complex.

	Washed out percentage	Elution Efficiency
0.1 mM Cu(II)-YGGFL	46.8 %	46.8 %
0.2 mM Cu(II)-YGGFL	29.8 %	40.6 %

As shown in Table 2, most of the Cu(II)-YGGFL complex was adsorbed to the C18 resin while less than half of the complex were eluted from the resin. There are two possible reasons: first, the complex dissociation still occurs under neutral conditions; second, Cu(II)-YGGFL complex is not so hydrophobic as YGGFL, therefore, it cannot be washed out thoroughly. Accordingly, the derivatization solution was added to both "wash solution" and "elution solution" so that even though the Cu(II)-YGGFL complex dissociates, the eluted YGGFL can still react with Cu(II) solution to reform the complex. Moreover, buffer solution was added to both "wash solution" and "elution solution" to adjust the pH value to 10, at which the Cu(II)-YGGFL complex is stable.

2.3.3 Condition 3

The new "wash solution" and "elution solution" are 0.024 M Na_2CO_3 & 0.0048 M $NaHCO_3$ buffer, and a 1: 1: 2 mixture of Cu(II) solution, the new wash solution and ACN, respectively. The results are illustrated in Table 3.

Table 3. The washed out percentage and elution efficiency of Cu(II)-YGGFL complex.

	Washed out percentage	Elution Efficiency
0.1 mM Cu(II)-YGGFL	46.4 %	78.6 %
0.2 mM Cu(II)-YGGFL	31.8 %	42.8 %

From Table 3, it is clear that there is only a little improvement after the addition of the buffer, which means that the complex is not that unstable under the neutral conditions and the relatively low elution efficiency is due to the low hydrophobicity of the Cu(II)-YGGFL complex.

2.3.4 Summary

All in all, although optimization of the experiment conditions are still required, we have shown that the Ziptip® pipette tips do adsorb the Cu(II)-peptide complex, and the complex can also be desorbed by organic solvent with considerable eluted fraction. As a result, it can be applied in the interface of the LC-CE system.

3.0 EFFECT OF TEMPERATURE ON DIFFUSION COEFFICIENT

3.1 BACKGROUND

3.1.1 Different methods in determination of diffusion coefficient

As mentioned in Chapter 1, diffusion coefficient is a very important factor in HPLC. Many researchers have made tremendous contributions to determine the diffusion coefficients.

As early as 1850, the diffusion coefficient was measured by Graham.[62] To date, a number of methods[49, 63-65] have been widely used for the accurate determination of diffusion coefficients. One example is the Aris-Taylor open tube method, which was introduced by Wakeham[66] and Kikta[67] in 1974. In this method, a small amount of sample is injected into a long tube to achieve steady-flow. The diffusion coefficient was hence calculated through the dispersion of the sample as it leaves the tube. The advantage of this method is that it is an absolute method which requires no calibration, and it works best for near infinite dilution. However, the reported methods for the diffusion coefficient determination are quite complicated.

Besides measuring diffusion coefficients experimentally, diffusion coefficients can also be estimated by a few empirical equations, such as Wilke-Chang equation[68] and others[69-72]. The problem is, the accuracy of these empirical equations is doubtful.

Therefore, a simple method, which was developed by Beisler et al.[73] in our laboratory, has been used in this experiment to evaluate the accuracy of these empirical equations.

3.1.2 Theory for our experiment

According to the plate height theory[11], the plate height in units of time, H_t has the following relationship with the plate height in units of length, H_L:

$$H_L = \sigma_l^2 / L = (\sigma_t^2 / t) \cdot v \tag{8}$$

In Equation 8, σ_L^2 and σ_t^2 represent the second central moments in units of length and time, respectively. L and t are the distance and time that the band travelled. And v is the linear velocity of the solute.

Also, as shown in Equation 9, plate height is related to the solute dispersion coefficient, D:

$$H_L = 2 \cdot D / v \tag{9}$$

Moreover, solute dispersion coefficient, D is related to molecular diffusion coefficient, D_{mol}, as displayed in Equation 10:

$$D = v^2 \cdot a^2 / 48 \cdot D_{mol} \tag{10}$$

As a result,

$$\sigma_t^2 = \frac{a^2}{24 \cdot D_{mol}} \cdot t \tag{11}$$

Based on Equation 11, when the second central moment σ_t^2 is plotted against the first central moment t, the slope equals to $\frac{a^2}{24 \cdot D_{mol}}$, which can be used to calculate D_{mol}.

3.2 MATERIALS AND METHODS

3.2.1 Materials

All the reagents used in this experiment, including the organic solvent ACN, trifluoroacetic acid (TFA) and all the peptides, such as Insulin (from Bovine pancreas), Insulin B chain (oxidized from Bovine insulin pancreas), Gly-Phe, *etc*., were purchased from Sigma (St. Louis, MO). ACN and TFA are of chromatography grade and analytical grade, respectively. Water for all studies was purified with Milli-Q system (Millipore Synthesis A10, Billerica, MA). Peptides were dissolved in 0.1 % TFA in milli-Q water at 2 mg/mL. The mobile phase and the peptide solutions are all filtered with 0.1 μm nylon filters (Cameo 25NS) prior to use.

In addition, two compositions of mobile phases were utilized: mobile phase 1 (0.1 % TFA in 50:50 ACN/milli-Q water) and mobile phase 2 (0.1 % TFA in 25:75 ACN/milli-Q water).

3.2.2 Experimental conditions

In our experiment, a large volume sample is injected to produce a steady-state signal. In addition, several parameters, such as temperature, the linear velocity of the fluid, and capillary diameter and length, are controlled to ensure diffusion in the Taylor regime, which is determined by the Peclet number ($P_e = v_r \cdot a_r / D_r$) and the capillary diameter and length[74].

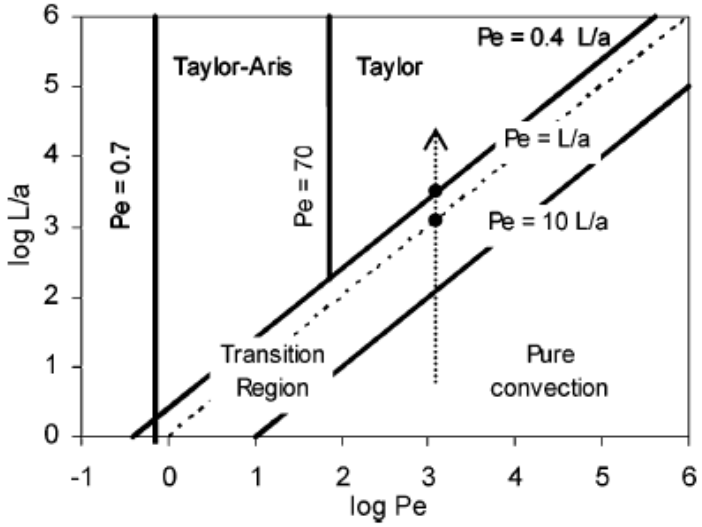

Figure 9. Taylor regime[74].

As shown in Figure 9, to be in the Taylor regime, two conditions: $\log P_e > 1.8$ and $L/a > 2.5 \cdot P_e$, have to be satisfied. In our system, P_e ranges from 150 to 2000, and L/a equals to 25680, which is much higher than $2.5 \cdot P_e$. Therefore, the diffusion in this experiment does perform in the Taylor regime.

3.2.3 Experiment Set-up and data treatment

Three different flow rates (1 $\mu L/\min$, 2 $\mu L/\min$ and 3 $\mu L/\min$) were controlled by a syringe pump (Harvard, Holliston, MA), while five different temperatures (25 $^{\circ}C$, 30 $^{\circ}C$, 40 $^{\circ}C$, 60 $^{\circ}C$ and 75 $^{\circ}C$) were set by two home-made temperature controllers (Minco, Minneapolis, MA) which control the temperature of the injector (model: EM2M28954, VICI, Houston, TX) and the capillary.

3.2.4 UV detector

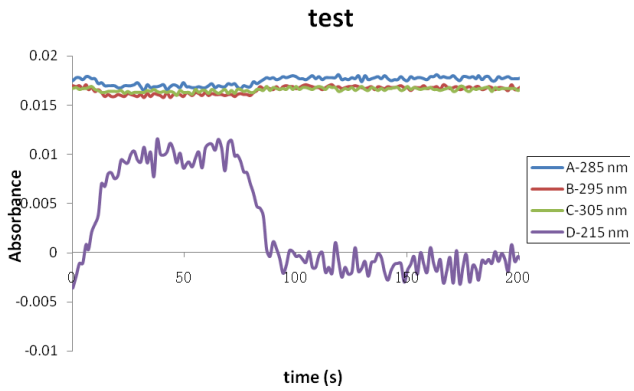

Figure 10. (a) UV signal of Insulin B Chain (Ocean Optics); (b) Relationship between the second central moment and first central moment for analytes that have passed through the capillaries from the injector to the detector.

The samples were initially detected by USB4000 miniature fiber optic spectrometer (Ocean optics). Figure 10 shows an example of the chromatogram of the insulin B chain solution (concentration: 2.0 mg/mL). As shown in the figure, there is detectable UV absorbance for

insulin B chain at wavelength 215 nm. However, the baseline is so noisy that very bad detection efficiency was obtained.

Therefore, better detectors are required, and we replaced the Ocean optics with the UV detector in Capillary Electropherograph (ISCO, model 3850). The samples were detected at 215 nm and the signal was collected by Peaksimple 3.29 (SRI Inc.). As illustrated in Figure 11, the sensitivity is greatly enhanced compared to the results obtained with Ocean Optics.

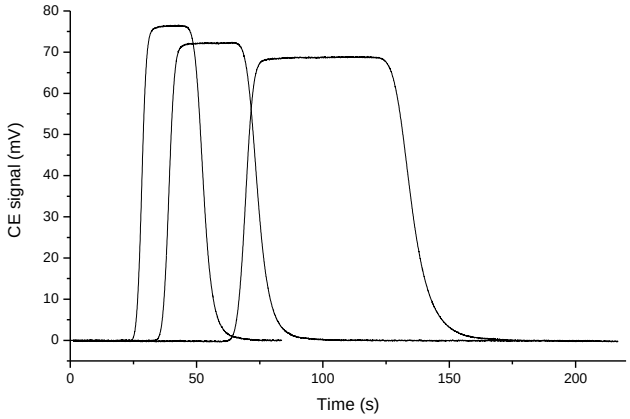

Figure 11. UV signal of Insulin Chain B at three different flow rates (UV detector 2).

3.2.5 Data processing

The data were imported into Origin 7.5 (OriginLab Cooperation) for differentiation, followed by the determination of the first and second central moments using PeakFit version 4 (AISN Software, Inc.). A linear plot of second moment versus first moment was made, an example of which is illustrated in Figure 12. The diffusion coefficient of the peptide was hence calculated

based on the slope of the plot ($D_{mol} = \frac{a^2}{24 \cdot slope}$). In addition, the errors for the diffusion coefficient were calculated based on the errors of the slope, assuming that there is no error in the flow rate, capillary length and capillary diameter.

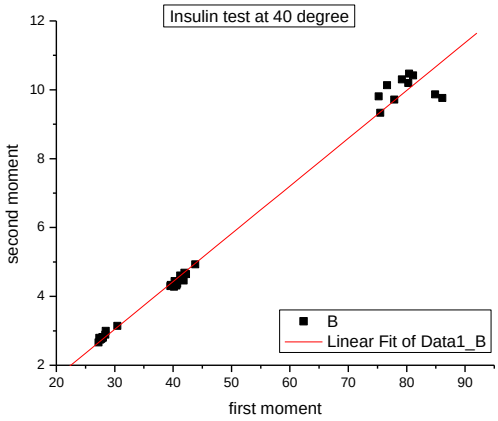

Figure 12. Relationship between the second central moment and first central moment for Insulin at 40 $^{\circ}C$.

3.3 RESULTS

During the experiment, 4 different peptides: Gly-Phe, Phe-Phe, Insulin and Insulin B chain were studied.

3.3.1 Diffusion coefficient with different mobile phase composition

It is predicted that when the viscosity of the mobile phase increases, the diffusion coefficient of the solute increases as well. As shown in Table 4, the experimentally determined diffusion coefficient for Insulin does show the same trend as predicted since mobile phase 1 (50: 50 ACN/milli-Q water) has lower viscosity than mobile phase 2 (25: 75 ACN/milli-Q water).

Table 4. Diffusion coefficients of Insulin at different temperatures.

$T/^{\circ}C$	Diffusion Coefficient			
	50: 50 ACN/milli-Q water		25: 75 ACN/milli-Q water	
	$D_{mol} \cdot 10^6 / cm^2/s$	$Error \cdot 10^6 / cm^2/s$	$D_{mol} \cdot 10^6 / cm^2/s$	$Error \cdot 10^6 / cm^2/s$
24	1.79	0.03	1.37	0.03
40	2.30	0.09	1.88	0.04

3.3.2 Diffusion coefficient with different temperatures

As discussed in previous context, the diffusion coefficient of peptides increases with temperature. And the results of diffusion coefficients of peptides at different temperatures are summarized as follows:

1. Results for Gly-Phe

Table 5. Diffusion coefficients of Gly-Phe at different temperatures.

$T/^{\circ}C$	Diffusion Coefficient	
	$D_{mol}/10^{-6} \cdot cm^2 \cdot s^{-1}$	$Error/10^{-6} \cdot cm^2 \cdot s^{-1}$
24	5.13	0.10
30	5.50	0.13
40	6.15	0.14
60	9.01	0.28
75	11.4	0.46

2. Results for Phe-Phe

Table 6. Diffusion coefficients of Phe-Phe at different temperatures.

$T/^{\circ}C$	Diffusion Coefficient	
	$D_{mol}/10^{-6} \cdot cm^2 \cdot s^{-1}$	$Error/10^{-6} \cdot cm^2 \cdot s^{-1}$
26	5.14	0.23
30	5.46	0.13
40	6.34	0.13
60	9.86	0.26
75	12.08	1.49

3. Results for Insulin

Table 7. Diffusion coefficients of Insulin at different temperatures.

$T/^{\circ}C$	Diffusion Coefficient	
	$D_{mol}/10^{-6} \cdot cm^2 \cdot s^{-1}$	$Error/10^{-6} \cdot cm^2 \cdot s^{-1}$
24	1.37	0.03
30	1.44	0.04
40	1.88	0.04
60	2.23	0.03
75	2.30	0.14

4. Results for insulin B chain

Table 8. Diffusion coefficients of Insulin B chain at different temperatures.

$T/^{\circ}C$	Diffusion Coefficient	
	$D_{mol}/10^{-6} \cdot cm^2 \cdot s^{-1}$	$Error/10^{-6} \cdot cm^2 \cdot s^{-1}$
26	5.14	0.23
30	5.46	0.13
40	6.34	0.13
60	9.86	0.26
75	12.08	1.49

3.4 DISCUSSION

3.4.1 Empirical equations

The diffusion coefficients of peptides can be estimated by several empirical equations, which are summarized as follows:

1. Stokes-Einstein equation

$$D_m = \frac{RT}{6r\eta N_{Av}} \tag{5}$$

In this equation, R and N_{Av} are the gas constant and Avogodro's number, T represents the temperature of the system (K), r stands for the hydrodynamic radius of the diffusion molecule (assumed spherical), and η represents viscosity of the solvent ($kg \cdot m^{-1} \cdot s^{-1}$).

2. Wilke-Chang Estimation Method[67]

$$D_{A,B}(cm^2/s) = 7.4\times10^{-8} \cdot \frac{\sqrt{\psi_B MW_B} \cdot T}{\eta_B \bar{V}_A^{0.6}} \tag{12}$$

In this equation, A and B represent solute and solvent, respectively. $\bar{V}_A$ is the molar volume (mL/mol) of the liquid solute at its normal boiling point. MW_B, η_B and ψ_B represent the molecular weight (g/mol), viscosity (cP) and solvent/solvent interaction coefficient (1 for nonassociated solvents, 1.5 for ethanol, 1.9 for methanol, 2.6 for water) of the solvent. T stands for the temperature of the system.

3. Scheibel Correlation[71]

$$D_{A,B}(cm^2/s) = \frac{A_S T}{\eta_B \bar{V}_A^{1/3}} \cdot \left[1 + \left(\frac{3\bar{V}_B}{\bar{V}_A} \right)^{2/3} \right] \tag{13}$$

In this equation, $\bar{V}_B$ is the molar volume of the solvent (mL/mol), A_S is a constant which equals to 8.2×10^{-8}. All other symbols are the same as those in Equation 8.

4. Reddy-Doraiswamy Correlation[70]

$$D_{A,B}(cm^2/s) = \frac{K' \cdot \sqrt{MW_B} \cdot T}{\eta_B (\bar{V}_A \bar{V}_B)^{1/3}} \tag{14}$$

In this equation, $K' = 10\times10^{-8}$ $\qquad \bar{V}_B / \bar{V}_A \le 1.5$

$K' = 8.5\times10^{-8}$ $\qquad \bar{V}_B / \bar{V}_A \ge 1.5$

All other symbols are the same as those in Equation 12 and 13.

5. Lusis-Ratcliff Correlation[69]

$$D_{A,B}(cm^2/s) = \frac{8.52\times10^{-8} \cdot T}{\eta_B \bar{V}_B^{1/3}} \cdot \left[1.40 \cdot (\frac{\bar{V}_B}{\bar{V}_A})^{1/3} + \frac{\bar{V}_B}{\bar{V}_A} \right] \tag{15}$$

All other symbols are the same as those in Equation 12 and 13.

6. Hayduk-Laudie Correlation[68]

$$D_{A,B}(cm^2/s) = 13.26\times10^{-5} \cdot \eta_B^{-1.4} \cdot \bar{V}_A^{-0.589} \tag{16}$$

All other symbols are the same as those in Equation 12 and 13.

3.4.2 Comparison of experimental values versus estimation value by empirical equations

1. Gly-Phe

As displayed in Figure 13, the five navy dots represent experimentally determined diffusion coefficients of Gly-Phe, and six different colored lines stand for the estimation value from six empirical equations. It seems that among the six equations, Stokes-Einstein equation and Scheibel correlation work better than the other equations. In addition, the relative error compared to the experimental values is illustrated in Figure 14. The relative error for Stokes-Einstein equation and Scheibel correlation is within 25 % and 37 %, respectively.

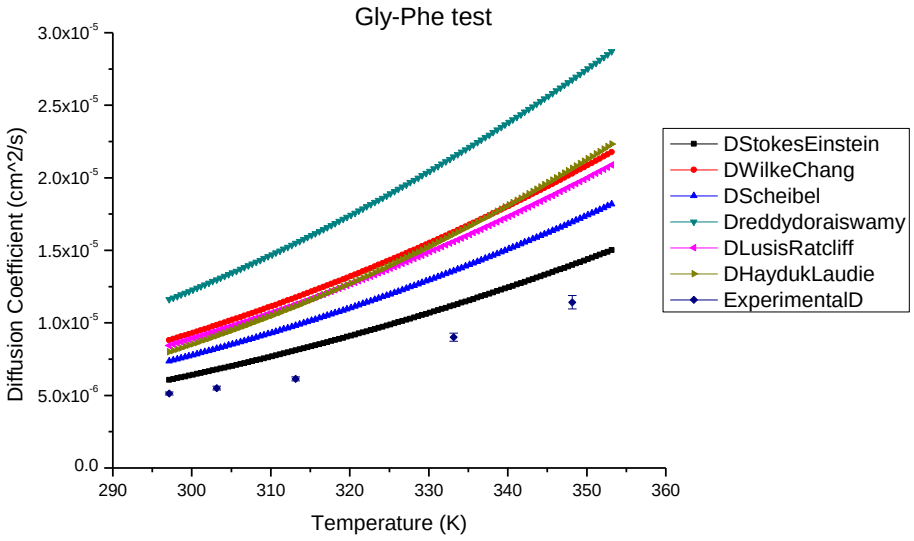

Figure 13. Experimental diffusion coefficients of Gly-Phe versus estimation value by empirical equations.

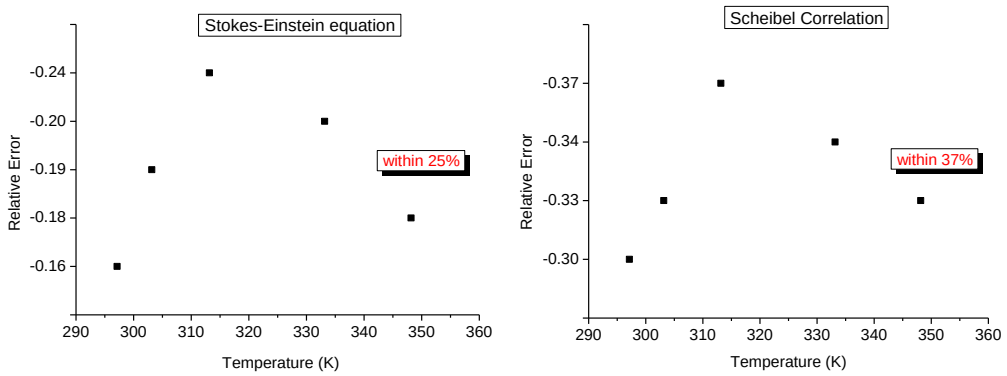

Figure 14. Relative error between (a) Stokes-Einstein equation (b) Scheibel correlation and experimental value.

2. Phe-Phe

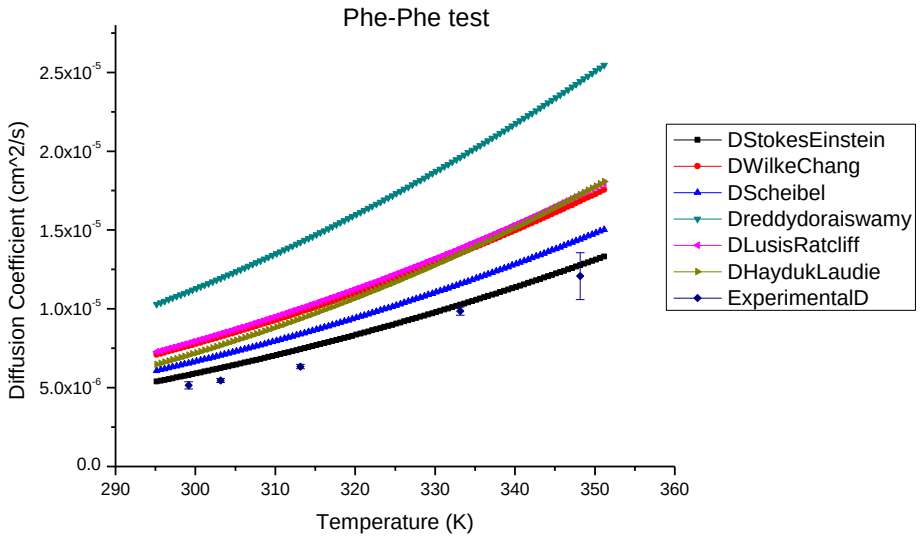

Figure 15. Experimental diffusion coefficients of Phe-Phe versus estimation value by empirical equations.

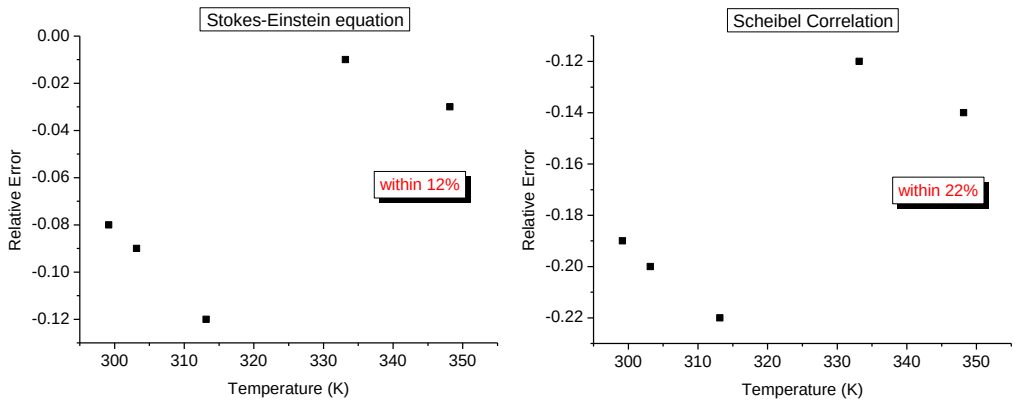

Figure 16. Relative error between (a) Stokes-Einstein equation (b) Scheibel correlation and experimental value.

As shown in Figure 15, the five navy dots represent experimentally obtained diffusion coefficients of Phe-Phe, and six different colored lines stand for the estimation value from the six empirical equations. Similar to Gly-Phe, Stokes-Einstein equation and Scheibel correlation, with relative error of within 12 % and 22 % (shown in Figure 16), perform better than other correlations in the case of Phe-Phe.

3. Insulin

As shown in Figure 17, the experimental values are plotted together with the estimation values from empirical equations. Similar to Gly-Phe and Phe-Phe, the Stokes-Einstein equation and Scheibel correlation give satisfactory results for insulin. Moreover, Lusis-Ratcliff correlation also works well in this case.

The fact that insulin is rather considered as a small protein is a possible reason for its slightly different behavior from the small peptides (Gly-Phe and Phe-Phe). In addition, the hydrodynamic radius of insulin is obtained from its crystal structure, while those of other

peptides are obtained at http://www.molinspiration.com/. The different sources of hydrodynamic radius may also account for why insulin behaves differently from other peptides.

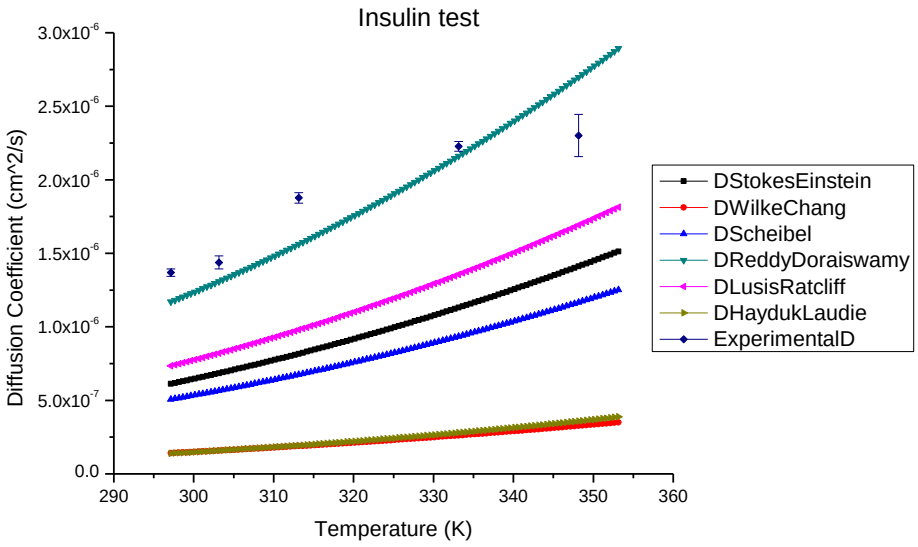

Figure 17. Experimental diffusion coefficients of Insulin versus estimation value by empirical equations.

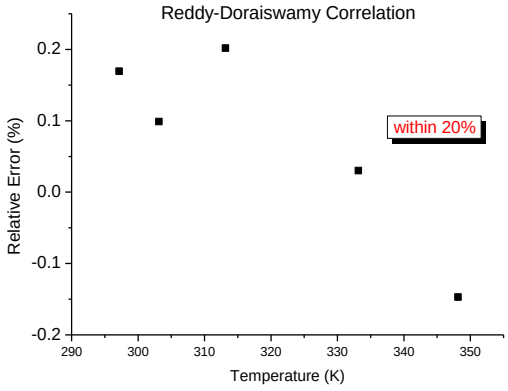

Figure 18. Relative error between Reddy-Doraiswamy correlation and experimental value.

Furthermore, it is worth noting from Figure 17 that when the temperatures are lower than 333.15 K, the diffusion coefficient increases with temperature. However, at 348.15 K, the diffusion coefficient wasn't as high as expected. From Bohidar's research work, it is suggested that insulin tends to aggregate at high temperature and under acidic conditions.[75] Since the mobile phase is acidic, it is possible that insulin aggregates or denatures at high temperature, which results in larger hydrodynamic radius. As a result, the diffusion coefficient is smaller than expected. The relative errors of those correlations in the temperature range of 298.15K and 333.15 K are shown in Figure 18.

4. Insulin B chain

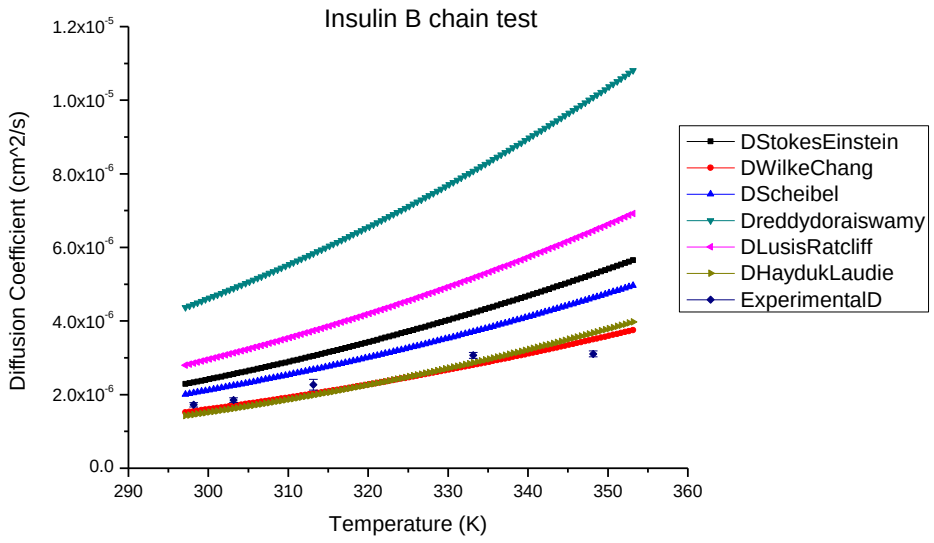

Figure 19. Experimental diffusion coefficients of Insulin B chain versus estimation value by empirical equations.

For Insulin B chain, which is a large peptide, the relationship between the experimental value and estimation value is slightly different from that for the small peptides, such as Gly-Phe

and Phe-Phe. In this case, besides Scheibel correlation and Stokes-Einstein equation, two more correlations: Hayduk-Laudie correlation and Wilke-Chang correlation fit better than the other correlations. (Figure 19)

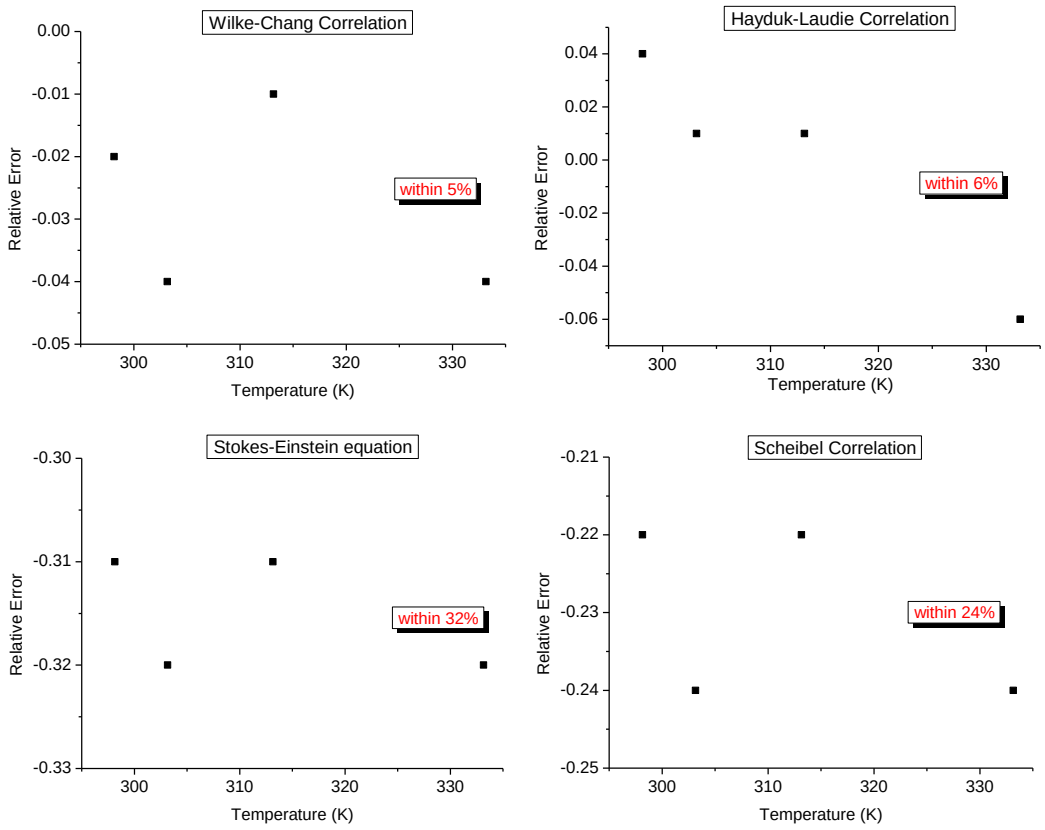

Figure 20. Relative error between (a) Wilke-Chang correlation (b) Hayduk-Laudie correlation (c) Stokes-Einstein equation and (d) Scheibel correlation and experimental value.

In addition, similar to Insulin, the diffusion coefficient of Insulin B chain increases with temperature when temperature is below 333.15 K, and flattens out at 348.15 K. The possible reason is that insulin B chain may also aggregate or denature at high temperature. The relative errors for Insulin B chain in the temperature range of 298.15K and 333.15 K are illustrated in

Figure 20, which are within 5%, 6 %, 32 % and 24 % for Wilke-Chang correlation, Hayduk-Laudie Correlation, Stokes-Einstein equation and Scheibel correlation, respectively.

3.4.3 Hydrodynamic radius

The current results suggest that the accuracy of the empirical equations is dependent on the accuracy of hydrodynamic radius which is used in those calculations. Therefore, we utilized the experimentally obtained diffusion coefficients and Stokes-Einstein equation to calculate the hydrodynamic radius at different temperatures. The results are summarized in Table 9.

Table 9. Hydrodynamic radius of peptides at various temperatures.

Peptides	*Hydrodynamic radius* $/ 10^{-10} \cdot m$					
	Used in the calculation	298 K	303 K	313 K	333 K	348 K
Insulin	18.6[a]	16.2	17.2	15.7	18.4	22.2
Insulin B chain	9.70[b]	13.1	13.4	13.0	13.3	16.6
Gly-Phe	3.65[b]	4.32	4.51	4.81	4.55	4.48
Phe-Phe	4.12[b]	4.48	4.54	4.67	4.15	4.23

Note: a – hydrodynamic radius is calculated from crystal structure;

b – hydrodynamic radius is obtained from http://www.molinspiration.com/.

As mentioned before, the hydrodynamic radius of insulin is calculated from its crystal structure while those of insulin B chain, Gly-Phe and Phe-Phe are obtained from http://www.molinspiration.com. The different sources of hydrodynamic radius could introduce errors in evaluating the hydrodynamic radius of empirical equations. From Table 9, it is obvious that the hydrodynamic radius of Insulin used in the empirical equation calculations significantly deviates from the values calculated with Stokes-Einstein equation.

It is also notable that though the hydrodynamic radius of the peptides is close to the radius used in the empirical equation calculations, there are still some differences between them. This is probably due to the non-spherical shape of the peptides since the hydrodynamic radius used in the empirical equation calculations are calculated by the volume of the molecules and the relationship between the radius and volume of a sphere. As a result, the hydrodynamic radius is not that accurate. Another possible reason is the hydration of the peptides, which leads to higher experimentally obtained hydrodynamic radius than the estimated value.

3.4.4 Summary

From the current information we have obtained, both Stokes-Einstein equation and Scheibel correlation seem to work for the tested peptides. Although the relative error is still large (overall within 32% and 43%, respectively), they perform better than all the other correlations. In addition, for some peptides such as Gly-Phe and Phe-Phe, Stokes-Einstein equation works even better than Scheibel correlation. We still need to do more experiments in order to test whether Stokes-Einstein equation and Scheibel correlation will work for other peptides as well. In addition, more work need to be carried out in order to find a better way to estimate the

hydrodynamic radius of peptides, which will provide more accurate estimation values from empirical equations.

4.0 FUTURE WORK

4.1 LC-CE INTERFACE

As discussed previously, the elution efficiency of Cu(II)-YGGFL complex under the current conditions are not good enough. If it is used in the LC-CE interface, comprehensive LC-CE separation will be difficult to actualize due to the considerable resolution loss in the interface. Therefore, optimization of the conditions must be performed to achieve higher eluted fraction. In addition, since the previous study is rather considered as an off-line detection, an on-line detection (Figure 21) will be performed to examine whether the C18 resin can be used in the interface.

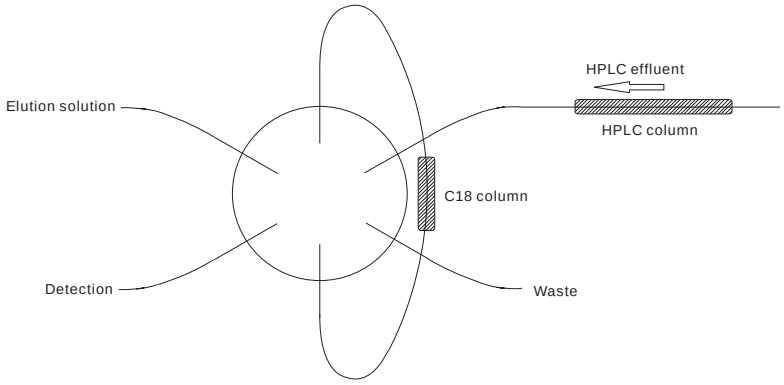

Figure 21. Schematic view of the on-line detection.

4.2 BATTERY-OPERATED POTENTIOSTAT

In the above context, methods to isolate the separation current with the detection signal are discussed. In our experiment, we would like to use the electrically isolated potentiostat developed by Lunt's group. A battery-operated potentiostat is currently under construction in electronic shop. With the potentiostat, we will test whether it can efficiently separate the separation voltage from the detection current of the electrochemical detection of the CE system.

4.3 CHIP ELECTROPHORESIS

Chips for electrophoresis are made in University of Virginia. (Figure 23) Experiments will be performed together with the battery-operated potentiostat for separation of peptides.

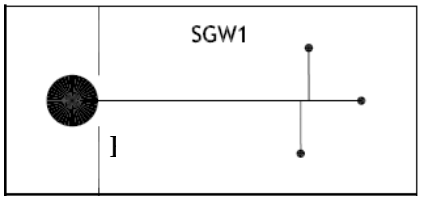

Figure 22. Schematic of the chip.

4.4 DIFFUSION COEFFICIENT DETERMINATION

An autosampler (Hewlett-Packard) will be programmed and attached to the injector, so that automatic injections can be realized. In addition, more peptides, such as Neurotensin 1-8 and substance B, will be studied. With the diffusion coefficients of a series of peptides, we may be able to add a correction coefficient into a specific correlation so that it can work for all the peptides.

BIBLIOGRAPHY

(1) Jerkovich, A. D.; Mellors, J. S.; Jorgenson, J. W. *LC-GC N. Am.* 2003, *21*, 600, 604, 606, 608, 610.

(2) Shen, Y.; Zhao, R.; Berger, S. J.; Anderson, G. A.; Rodriguez, N.; Smith, R. D. *Anal. Chem.* 2002, *74*, 4235-4249.

(3) Shen, Y.; Moore, R. J.; Zhao, R.; Blonder, J.; Auberry, D. L.; Masselon, C.; Pasa-Tolic, L.; Hixson, K. K.; Auberry, K. J.; Smith, R. D. *Anal. Chem.* 2003, *75*, 3596-3605.

(4) Chen, H.; Horvath, C. *J. Chromat. A* 1995, *705*, 3-20.

(5) Consden, R. G., A. H.; Martin, A. J. P *Biochem. J.* 1944, *38*, 224-232.

(6) Haugaard, G.; Kroner, T. D. *J. Am. Chem. Soc.* 1948, *70*, 2135-2137.

(7) Durrum, E. L. *J. Colloid Sci.* 1951, *6*, 274-290.

(8) Giddings, J. C. *Anal. Chem.* 1967, *39*, 1027-1028.

(9) O'Farrell, P. H. *J. Biol. Chem.* 1975, *250*, 4007-4021.

(10) Guiochon, G.; Gonnord, M. F.; Zakaria, M.; Beaver, L. A.; Siouffi, A. M. *Chromatographia* 1983, *17*, 121-124.

(11) Giddings, J. C. *Unified Separation Science*, 1991.

(12) Bushey, M. M.; Jorgenson, J. W. *Anal. Chem.* 1990, *62*, 161-167.

(13) Cortes, H. J. *Multidimensional Chromatography: techniques and application. Marcel Dekker, New York* 1990.

(14) Murphy, R. E.; Schure, M. R.; Foley, J. P. *Anal. Chem.* 1998, *70*, 1585-1594.

(15) Sonnefeld, W. J.; Zoller, W. H.; May, W. E.; Wise, S. A. *Anal. Chem.* 1982, *54*, 723-727.

(16) Nakanishi, K.; Soga, N. *J. Am. Ceram. Soc.* 1991, *74*, 2518-2530.

(17) Nakanishi, K.; Soga, N. *J. Non-Cryst. Solids* 1992, *139*, 1-13.

(18) Nakanishi, K. *J. Porous Mater.* 1997, *4*, 67-112.

(19) Motokawa, M.; Kobayashi, H.; Ishizuka, N.; Minakuchi, H.; Nakanishi, K.; Jinnai, H.; Hosoya, K.; Ikegami, T.; Tanaka, N. *J. Chromat. A* 2002, *961*, 53-63.

(20) Thompson, J. D.; Carr, P. W. *Anal. Chem.* 2002, *74*, 1017-1023.

(21) Greibrokk, T.; Andersen, T. *J. Chromat. A* 2003, *1000*, 743-755.

(22) Vanhoenacker, G.; Sandra, P. *J. Chromat. A* 2005, *1082*, 193-202.

(23) Yan, B.; Zhao, J.; Brown, J. S.; Blackwell, J.; Carr, P. W. *Anal. Chem.* 2000, *72*, 1253-1262.

(24) Lestremau, F.; Cooper, A.; Szucs, R.; David, F.; Sandra, P. *J. Chromat. A* 2006, *1109*, 191-196.

(25) Bonincontro, A.; Risuleo, G. *Spectrochim. Acta, Part A* 2003, *59A*, 2677-2684.

(26) Holland, L. A.; Jorgenson, J. W. *Anal. Chem.* 1995, *67*, 3275-3283.

(27) Stroink, T.; Paarlberg, E.; Waterval, J. C. M.; Bult, A.; Underberg, W. J. M. *Electrophoresis* 2001, *22*, 2374-2383.

(28) Chien, W.-J.; Cheng, S.-F.; Chang, D.-K. *Anal. Biochem.* 1998, *264*, 211-215.

(29) Jorgenson, J. W.; Lukacs, K. D. *Anal. Chem.* 1981, *53*, 1298-1302.

(30) Gassmann, E.; Kuo, J. E.; Zare, R. N. *Science* 1985, *230*, 813-814.

(31) Liu, Y.-M.; Sweedler, J. V. *Anal. Chem.* 1996, *68*, 3928-3933.

(32) Lemmo, A. V.; Jorgenson, J. W. *Anal. Chem.* 1993, *65*, 1576-1581.

(33) Rossier, J. S.; Ferrigno, R.; Girault, H. H. *J. Electroanal. Chem.* 2000, *492*, 15-22.

(34) Osbourn, D. M.; Lunte, C. E. *Anal. Chem.* 2003, *75*, 2710-2714.

(35) Martin, R. S.; Ratzlaff, K. L.; Huynh, B. H.; Lunte, S. M. *Anal. Chem.* 2002, *74*, 1136-1143.

(36) Bushey, M. M.; Jorgenson, J. W. *Anal. Chem.* 1990, *62*, 978-984.

(37) Bushey, M. M., Jorgenson, James W. *J. Microcolumn Sep.* 1990, *2*, 293-299.

(38) Martin, M.; Blu, G.; Eon, C.; Guiochon, G. *J. Chromatogr. Sci.* 1974, *12*, 438-448.

(39) Guiochon, G. *Anal. Chem.* 1980, *52*, 2002-2008.

(40) Knox, J. H.; Saleem, M. *J. Chromatogr. Sci.* 1969, *7*, 614-622.

(41) Poppe, H. *J. Chromat. A* 1997, *778*, 3-21.

(42) Antia, F. D.; Horvath, C. *J. Chromat.* 1988, *435*, 1-15.

(43) Synder, L. R.; Dolan, J. W.; Molnar, I.; Djordjevic, N. M. *LC-GC* 1997, *15*, 136, 136, 140, 142-144, 146, 148, 149-151.

(44) Thompson, J. D.; Carr, P. W. *Anal. Chem.* 2002, *74*, 4150-4159.

(45) Thompson, J. D.; Brown, J. S.; Carr, P. W. *Anal. Chem.* 2001, *73*, 3340-3347.

(46) MacNair, J. E.; Lewis, K. C.; Jorgenson, J. W. *Anal. Chem.* 1997, *69*, 983-989.

(47) Stoll, D. R.; Li, X.; Wang, X.; Carr, P. W.; Porter, S. E. G.; Rutan, S. C. *J. Chromat. A* 2007, *1168*, 3-43.

(48) Guillarme, D.; Heinisch, S.; Rocca, J. L. *J. Chromat. A* 2004, *1052*, 39-51.

(49) Li, J.; Carr, P. W. *Anal. Chem.* 1997, *69*, 2530-2536.

(50) Chloupek, R. C.; Hancock, W. S.; Marchylo, B. A.; Kirkland, J. J.; Boyes, B. E.; Snyder, L. R. *J. Chromat. A* 1994, *686*, 45-59.

(51) Goga-Remont, S.; Heinisch, S.; Lesellier, E.; Rocca, J. L.; Tchapla, A. *Chromatographia* 2000, *51*, 536-544.

(52) Li, J. *Anal. Chim. Acta* 1998, *369*, 21-37.

(53) Poppe, H.; Kraak, J. C.; Huber, J. F. K.; Van den Berg, J. H. M. *Chromatographia* 1981, *14*, 515-523.

(54) Poppe, H.; Kraak, J. C. *J. Chromat.* 1983, *282*, 399-412.

(55) Wolcott, R. G.; Dolan, J. W.; Snyder, L. R.; Bakalyar, S. R.; Arnold, M. A.; Nichols, J. A. *J. Chromat. A* 2000, *869*, 211-230.

(56) Yang, X. *Ph. D. Thesis, University of Minnesota, Minneapolis* 2004.

(57) Rodriguez-Mozaz, S.; Lopez de Alda, M. J.; Barcelo, D. *J. Chromat. A* 2007, *1152*, 97-115.

(58) Puig, P.; Borrull, F.; Calull, M.; Aguilar, C. *TrAC, Trends Anal. Chem.* 2007, *26*, 664-678.

(59) Tamayo, F. G.; Turiel, E.; Martin-Esteban, A. *J. Chromat. A* 2007, *1152*, 32-40.

(60) Baggiani, C.; Anfossi, L.; Giovannoli, C. *Anal. Chim. Acta* 2007, *591*, 29-39.

(61) Cabooter, D.; Heinisch, S.; Rocca, J. L.; Clicq, D.; Desmet, G. *J. Chromat. A* 2007, *1143*, 121-133.

(62) Graham, T. *Phil. Trans.* 1850, *140*, 805.

(63) Wakeham, W. A. *Faraday Symposia of the Chemical Society* 1980, *15*, 145-154.

(64) Ouano, A. C. *Ind. Eng. Chem. Fundam.* 1972, *11*, 268-271.

(65) Atwood, J. G.; Goldstein, J. *J. Phys. Chem.* 1984, *88*, 1875-1885.

(66) Pratt, K. C.; Wakeham, W. A. *Proc. R. Soc. London, Ser. A* 1974, *336*, 393-406.

(67) Grushka, E.; Kikta, E. J., Jr. *J. Phys. Chem.* 1974, *78*, 2297-2301.

(68) Wilke, C. R.; Chang, P. *Am. Inst. Chem. Eng. J.* 1955, *1*, 264-270.

(69) Hayduk, W.; Laudie, H. *AIChE Journal* 1974, *20*, 611-615.

(70) Lusis, M. A.; Ratcliff, G. A. *Can. J. Chem. Eng.* 1968, *46*, 385-387.

(71) Reddy, K. A.; Doraiswamy, L. K. *Ind. Eng. Chem. Fundam.* 1967, *6*, 77-79.

(72) Scheibel, E. G. *J. Ind. Eng. Chem.* 1954, *46*, 2007-2008.

(73) Beisler, A. T.; Schaefer, K. E.; Weber, S. G. *J. Chromat. A* 2003, *986*, 247-251.

(74) Probstein, R. F. *Physicochemical Hydrodynamics, An Introduction: Second Edition*, 1994.

(75) Bohidar, H. B. *Biopolymers* 1998, *45*, 1-8.